International Journal of Scientific Research & Engineering Technology (IJSET)
Vol.7 pp. 48-55

A Novel Double Blumlein-Line Nitrogen Laser Circuit Analysis Based Distributed Parameters Model: Laser Source and Laser Amplifier

Mohamed O. Twati[#1], Mohammed N. Dorar[#2]

[#] *Electrical and Electronic Engineering Department, University of Tripoli*

[1]m.twati@uot.edu.ly

[2]M.Dorar@outlook.com

***Abstract*— In this paper, the analysis of a double Blumlein-line circuit that forms the oscillator – amplifier nitrogen laser system with one spark gap and based on a full-distributed parameter model is presented. The voltage, current and power waveforms outputs of the model are reported. The effect of the transmission line lengths, laser gap and spark gap parameters of the laser system on the output waveforms are studied and discussed. The simulation results presented here indicated that this analysis could be very useful and relatively more accurate than other models and techniques used for synchronization of the laser pulses between the laser oscillator and laser amplifier circuits. In addition this analysis is general and could be easily applied to study other laser systems such as metal vapour and carbon dioxide laser systems.**

***Keywords*— Blumlein-line; Fast discharge laser; Nitrogen laser; Laser amplifier; Pulse forming network.**

I. INTRODUCTION

Although extensive studies and investigations that have been made on oscillator-amplifier (OSC-AMP) nitrogen lasers, operating on the 337.1 nm transition of the second positive band system, aimed at determining the optimum synchronization time between the laser oscillator pulses and the laser amplifier [1]-[3], still a lot of work has to be made concerning this issue. This include the selection of more adequate system design, accurate circuit models for simulating the laser system and the effects of the electrical parameters on the overall laser performance. The double Blumlein-line N_2 laser circuit (DBL) consists of two Blumlein-line pulse forming networks with one spark gap. One of them is working as an oscillator whereas the other as an amplifier. The pulse forming network consists of two parallel plate transmission lines (or coaxial cables) acting as energy storage capacitors, located at both sides of the cavity charged to high voltage Vo. When one side is short circuited, for instance using a spark gap, a transient voltage occurs across the laser cavity creating a gas discharge between the electrodes. The spark gap and the laser gap are usually represented by resistances and inductances. For the DBL, first, the light pulses is injected from the OSC to the amplifier via a set of reflecting mirrors and the synchronization between the laser oscillator pulses and the laser amplifier could be accomplished experimentally by varying the AMP gas pressure appropriately to reach the synchronization time condition between OSC and AMP sections and /or using the modeling and simulation results of the laser system to estimate the synchronization time [3]. Also, the synchronization could be achieved by using two park gaps, one for the oscillator and the other for the amplifier, and using a precise triggering circuits to synchronize the oscillator output with the peak amplifier discharge current [2]. Using two spark gaps and trigger circuits for synchronization purpose could make the system more complex and might reduce the accuracy in obtaining the synchronization time. Two concepts can be used in the analysis and modeling of the double Blumlein-line circuit, the lumped parameter model (LPM) and the distributed parameter model (DPM). However, LPM has the disadvantage of being valid only when the transit time on the transmission line is much smaller than the relative time constants of the spark gap and laser gaps [4].

This paper presents the theoretical analysis, electrical and optical output waveforms and the effect of some circuit parameters on the laser system performance of the double Blumlein-line

ISSN 1737-9296

N_2laser circuit that based on the DPM and using only one spark gap.

II. The Double Blumlein-Line Differential Equations And Initial And Boundary Conditions

The schematic diagram and the mathematical configuration of the double Blumlein-line are shown in figures 1 and 2 respectively. For reasons of computational comfortability and simplifying the treatment with the mathematical model, the DBL is divided into four sections with three different zero coordinates. Two sections for each of the OSC and the AMP as shown in figure 2.

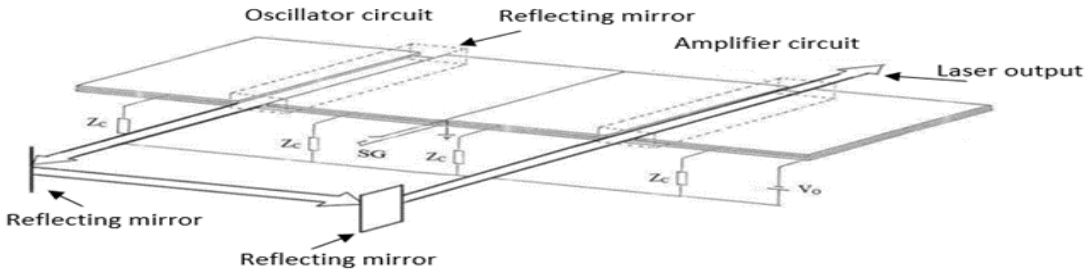

Figure 1. Schematic diagram of a transversely excited Blumlein circuit. Zc charging resistance; Vo: high voltage power supply; SG: spark gap.

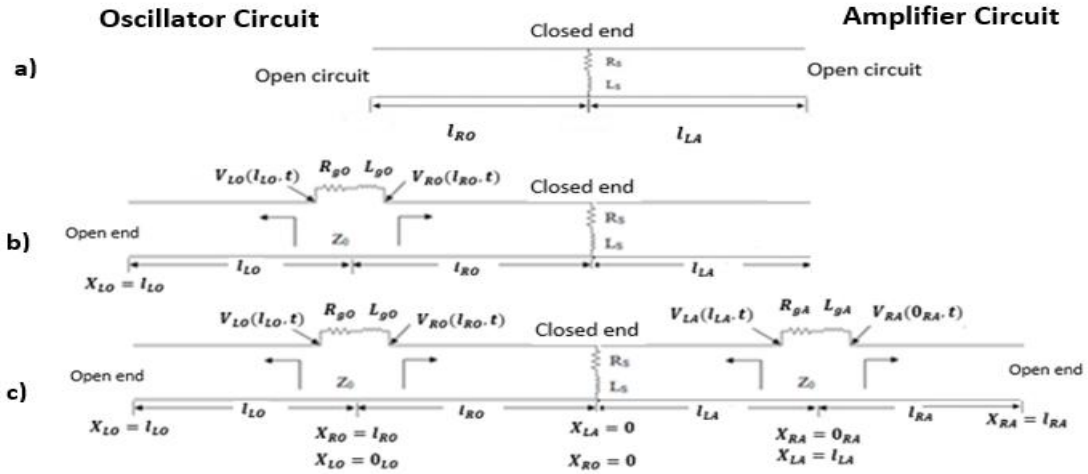

Figure 2. Mathematical configuration of the double Blumlein circuit. a): before breakdown of both OSC&AMP, b): after breakdown of OSC, c): after breakdown of both OSC& AMP; Zo: characteristic impedance.

For reasons of computational comfortability and simplifying the treatment with the mathematical model, the DBL is divided into four sections with three different zero coordinates. Two sections for

ISSN 1737-9296

each of the OSC and the AMP as shown in figure 2. The applicable partial differential equations for voltage V and current I on a section of transmission line of dx at any time t are given by,

$$\partial V_{ij}(x_{ij},t)/\partial x = -\bar{L}\,\partial I_{ij}(x_{ij},t)/\partial t \quad (1)$$

$$\partial I_{ij}(x_{ij},t)/\partial x = -\bar{C}\,\partial V_{ij}(x_{ij},t)/\partial t \quad (2)$$

where, $0_{ij} \le x_{ij} \le l_{ij}$, i = left (L) and right (R), and j = oscillator (O) and amplifier (A). $\bar{L}$ and $\bar{C}$ are the distributed inductance and capacitance per unit length respectively, and l is the total length of line section, where Z_o ($Z_o = \sqrt{\bar{L}/\bar{C}}$) is the characteristic impedance of the line. The initial conditions are:

$$V_{ij}(x_{ij},0) = Vo \quad (3)$$

$$I_{ij}(x_{ij},0) = 0 \quad (4)$$

At the spark gap side $x_{RO} = x_{LA} = 0_{Sp}$, where 0_{Sp} is the spark-gap zero coordinate. Hence, the voltage boundary conditions at the end of the spark-gap can be written as:

$$V_{LA}(x_{LA},t) = V_{RO}(x_{RO},t) = V_{Sp}(0_{Sp},t) \quad (5)$$

$$V_{Sp}(0_{Sp},t) = -R_S[I_{Sp}(0_{Sp},t) + \tfrac{L_S}{R_S}\partial I_{Sp}(0_{Sp},t)/\partial t\,] \quad (6)$$

And the current boundary conditions as well can be written as:

$$I_{LA}(x_{LA},t) + I_{RO}(x_{RO},t) = I_{Sp}(0_{Sp},t) \quad (7)$$

The boundary conditions at the oscillator channel are:

$$V_{RO}(l_{RO},t) - V_{LO}(0_{LO},t) = L_{go}\partial I_{LO}(0_{LO},t)/\partial t + R_{go}I_{LO}(0_{LO},t) \quad (8)$$

$$I_{RO}(l_{RO},t) = I_{LO}(0_{LO},t) \quad (9)$$

The boundary condition at the open end of the oscillator is:

$$I_{LO}(l_{LO},t) = 0 \quad (10)$$

(L_S and R_S) and (L_{go} and R_{go}) stand for inductances and resistors of the spark gap and laser gap of the oscillator, respectively.

Similarly, the boundary conditions for the amplifier section (amplifier channel & open end of the amplifier section) can be obtained just by interchanging the subscripts in the voltage and current equations of the oscillator by the amplifier subscripts. Therefore, the boundary conditions at the amplifier channel can be written as:

$$V_{LA}(l_{LA},t) - V_{RA}(0_{RA},t) = L_{gA}\partial I_{RA}(0_{RA},t)/\partial t + R_{gA}I_{RA}(0_{RA},t) \quad (11)$$

$$I_{RA}(0_{RA},t) = I_{LA}(l_{LO},t) \quad (12)$$

The boundary condition at the open end of the amplifier is:

$$I_{RA}(l_{RA},t) = 0 \quad (13)$$

where, L_{gA} and R_{gA} stand for the inductance and resistor of the amplifier laser gap respectively. The laser gap impedances in both the Oscillator and amplifier are not linear and must be treated as voltage dependent: as an open circuit before laser gaps breakdown and represented by a combination of (L_{go} & R_{go}) and (L_{gA} & R_{gA}) after laser gap breakdown. I_{Sp} is the current passed through the spark gap inductance and resistance. $I_{RO}(l_{RO},t)$ and $I_{RA}(0_{RA},t)$ are the currents passed in the channel inductances of the oscillator and the amplifier respectively after laser gaps breakdown. This nonlinear behavior of the channel impedances, makes it necessary, in the time development of solution of the partial differential equations (8) and (11) to distinguish between three time intervals: the first one is before laser gaps breakdown, during which the state of only the right-hand side of the oscillator circuit and the left-hand side of amplifier circuit subject to the dynamical changes, whereas the left-hand side of the oscillator and the right-hand side of the amplifier remain in their initial state. The second time interval is after oscillator laser gap breakdown, in which the states of both sides of the oscillator and the left-hand side of the amplifier are time varying whereas the right-hand side of the amplifier remains in its initial state. The third time interval is after amplifier laser gap breakdown, in which the states of all sides are time varying.

III. System of Equations for Optical Power Computation

ISSN 1737-9296

Equations for calculating the electrical waveforms behaviour (voltages and currents) of DBL have been derived and outlined in section 2. To obtain the equations that governing the temporal behaviour of the optical output power waveform of the DBL, two approaches can be utilized, the saturation approximation assumption and the general laser power assumption [5]. Here, the general laser power assumption is considered in calculating the output optical power.

According to Fitzsimmons' expression for relationship among the electron temperature, the instantaneous electric field E and the pressure P inside the laser channel [6], the electron density equation and the laser rate equations of the molecular nitrogen can be derived in term of (E/P). These equations are needed and will be used in obtaining the states densities and the optical output laser power. The Fitzsimmons' expression for the electron temperature, is given by [6]:

$$KT_e = 0.11(\mathrm{E/P})^{0.8} \quad (14)$$

The parameter *K* represents the Boltzmann's constant. The electron density equation can then be written as:

$$dn_e/dt = 4.06(10^{-3})n_e(\mathrm{E/P})^{4.7}\mathrm{P} \quad (15)$$

The laser rate equations are given by:

$$dN_C/dt = n_e N_o \sigma_{OC}(0.88/m\pi)^{0.5}(\mathrm{E/P})^{0.4} - \sigma_{Ostim}\, n_{ph} C(N_C - N_B) - N_C/\tau_C \quad (16)$$

$$dN_B/dt = n_e N_o \sigma_{OC}(0.88/m\pi)^{0.5}(E/P)^{0.4} + n_{ph} C(N_C - N_B) - N_B/\tau_B + N_C/\tau_C \quad (17)$$

$$dn_{ph}/dt = \sigma_{Ostim}\, n_{ph} C(N_C - N_B) - n_{ph}/\tau_{ph} + N_C/\tau_C \quad (18)$$

The electric field E is obtained from the voltage difference at the laser channels divided by channel electrodes separation *d* and can be written as:

$$[V_{RO}(l_{RO}, t) - V_{LO}(0_{LO}, t)]/d \quad (19)$$

All the above equations are applicable for both the oscillator and the amplifier sections, however, the subscripts in equation (19) should be changed for the amplifier section. n_e is the electron density, N_o ($\cong 3.2 \times 10^{16} P$) is the ground-state density which is assumed constant, τ_C is the radiative lifetime of the C-state (40ns) and τ_B is the radiative lifetime of the B-state (10μs). σ_{OC} is the electron impact cross section of the state C and equals to $11.1 \times 10^{-18} cm^2$, whereas σ_{OB} is the electron impact cross sections of the state B and equals $9.2 \times 10^{-18} cm^2$. N_C, N_B and n_{ph} are the number density of the C-state, the B-state, and the photons, respectively. τ_{ph} is the photon lifetime inside the laser tube. m is the electron mass (9.2×10^{-28}g) and C is the speed of light. σ_{Ostim} is the stimulated emission cross section ($4.5 \times 10^{-15} cm^2$). Upon obtaining the electron density n_e from equation (15), the above laser rate equations (16), (17) and (18) can then be solved.

IV. Selection Of The Finite Difference Schemes And Computational Procedure

The voltages and currents solutions across the laser channels of the oscillator and the amplifier of the DBL can be obtained by using numerical schemes that based on the finite difference method. These are the forward, backward and central difference schemes along-with the" Lax-wendroff scheme". The schemes are applied to the partial differential equations and the boundary conditions of the DBL [4]. Standard numerical techniques were also used in solving the laser rate equations and the electron density equation to obtain the optical power output waveforms.

In order to apply the above mentioned schemes to the coupled partial equations (1) & (2) and to the boundary conditions of the DBL, it is convenient to decouple and normalize them first. The normalized and decoupled equations can be written as [7].

$$U_t = SBU_x \quad (20)$$

where, *S* is the phase velocity in the transmission line, and

$U_t = \begin{pmatrix} \partial u_1/\partial t \\ \partial u_2/\partial t \end{pmatrix}, U_x = \begin{pmatrix} \partial u_1/\partial x \\ \partial u_2/\partial x \end{pmatrix}, B = \begin{pmatrix} -1 & 0 \\ 0 & 1 \end{pmatrix}, \quad u_1 = u + i,$ $u_2 = u - i, u = V(x_{ij}, t)\sqrt{C}$ and $i = I(x_{ij}, t)\sqrt{L}$.

Now, discretization procedure in time and space should be applied to the problem equations before the application of the Lax-Wendroff and other finite difference schemes. The notations for an approximate value of u($x_{ij,k}$, t_n) at each point

ISSN 1737-9296

$(x_{ij,k}, t_n)$ in space and time, of the discretized problem is usually written as:

$$u(x_{ij,k}, t_n) = U^n_{ij,k} \quad (21)$$

where, $\Delta x = x_{ij,k+1} - x_{ij,k}$ is the increment in space and $\Delta t = t_{n+1} - t_n$ is the increment in tine. The system of equations (1) & (2) under the application of the Lax-Wendroff scheme becomes:

$$U^{n+1} = U^n + \lambda B D^1_0(U^n) + 0.5\lambda^2 B^2 D^1_+ D^1_-(U^n) \quad (22)$$

$U^n = \begin{pmatrix} U^n_{1,ij,k} \\ U^n_{2,ij,k} \end{pmatrix}$, $\lambda = S\,\Delta x/\Delta t$ and the different operators D^1_0, D^1_+ and D^1_- are defined as follows:

$D^1_0(U^n_{ij,k}) = 0.5(U^n_{ij,k+1} - U^n_{ij,k-1})$, $D^1_+(U^n_{ij,k}) = (U^n_{ij,k+1} - U^n_{ij,k})$ and $D^1_-(U^n_{ij,k}) = (U^n_{ij,k} - U^n_{ij,k-1})$. The detailed process of the application of the Lax-Wendroff scheme can be found in previous work [3].

V. Computational Results And Discussions

Upon completion of the application of the numerical schemes mentioned in the previous section and simulation of the DBL laser system, useful results were obtained. The effect of the spark gap inductance are simulated and illustrated. The 3D-plot of the output waveforms of the voltage variation for (OSC-AMP) is presented to clarify the operation dynamics. The values of the circuit parameters used in the simulation (shown in Fig. 2) that used in the simulation are: $\bar{C}$ =128.88nF/m, $\bar{L}$= 0.288nH/m, $R_{gO} = R_{gA}$ = 0.1Ω, R_S = 0.0366Ω, $L_s = 13nH, l_{RO} = 0.2m, l_{LO} = 0.45m, l_{RA} = 0.45m,$ and $l_{LA} = 0.8m$. The parameter Z_o is obtained from the expression $Z_o = \sqrt{\bar{L}/\bar{C}}$. The chosen value of L_{gO} and L_{gA} for the simulation is 3.2nH. The electrodes separation used in the simulation is 0.015m whereas their lengths and widths are 0.3m and 0.005m respectively. The pressure inside the laser tube is considered to be about 82Torr. The peak value of (E/P) across the laser channels is taken to be in the range of 100 to 140V/cm.torr. The electrical power is obtained from the expression $(I^2 R_{gA})$ and $(I^2 R_{gO})$ whereas the optical power is estimated from (18). In the waveform figures, the time is normalized by the propagation time on the spark-gap side transmission-line of the oscillator $T_r = l_{RO}\sqrt{\bar{L}\,\bar{C}}$.
Figure 3 shows the voltage waveforms variations of the oscillator and the amplifier, whereas figure 4 shows the current waveform variations.

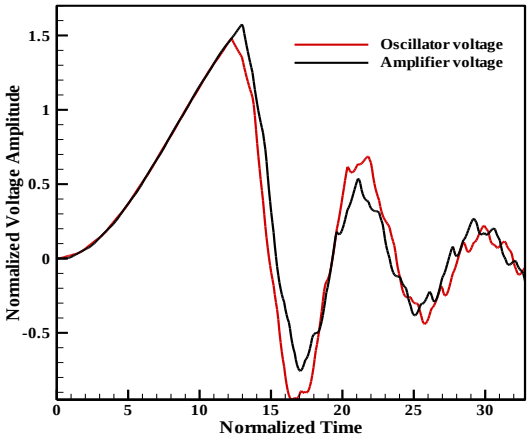

Figure 3. The laser channel voltages waveforms variations (OSC & AMP) with L_s = 13nH, $l_{RO} = 0.2m$ and $l_{LA} = 0.8m$.

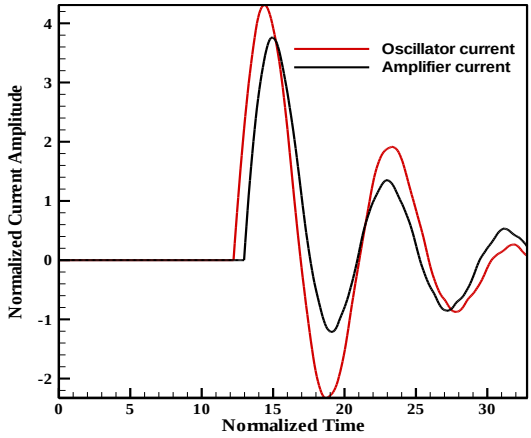

Figure 4. The laser channel currents waveforms variations (OSC & AMP) with L_s = 13nH, $l_{RO} = 0.2m$ and $l_{LA} = 0.8m$.

The effect of the transmission-line lengths on the current waveforms variations as well as to the time of the peak currents occurrences is shown in figure 5. It is clear that the increase of $(l_{RO} = 0.4m)$ and the decrease of $(l_{LA} = 0.6m)$ reduces the time difference between the peak currents occurrences of the oscillator and the amplifier. Also the transmission-line lengths has an effect on the time of starting current peaks. Hence, the synchronization time between (OSC-AMP) will be affected. The effect of the spark gap inductance and laser gaps inductance are shown in figures 6 and 7 respectively.

ISSN 1737-9296

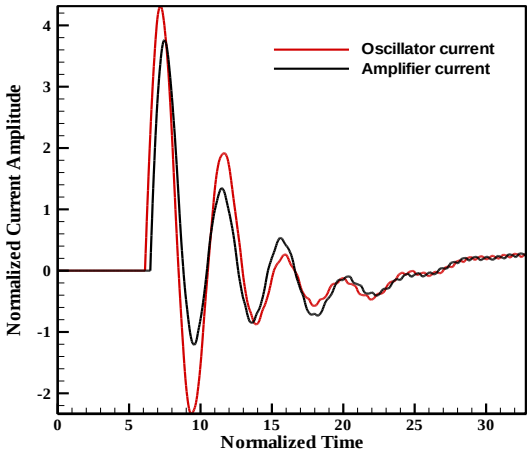

Figure 5. The laser channel currents waveforms variations (OSC & AMP) with L_s = 13nH, $l_{RO} = 0.4m$ and $l_{LA} = 0.6m$.

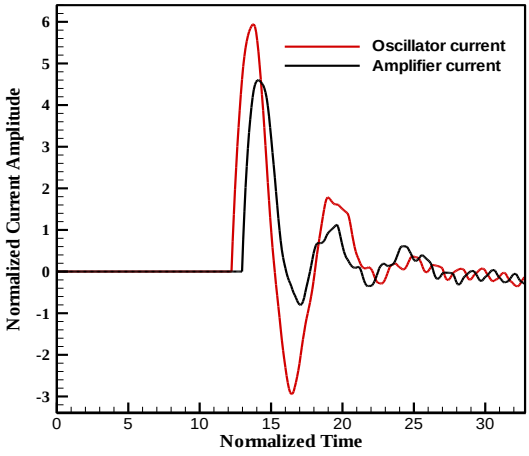

Figure 7. The laser channel currents waveforms variations (OSC & AMP) with L_g = 1.2nH, $l_{RO} = 0.2m$ and $l_{LA} = 0.8m$.

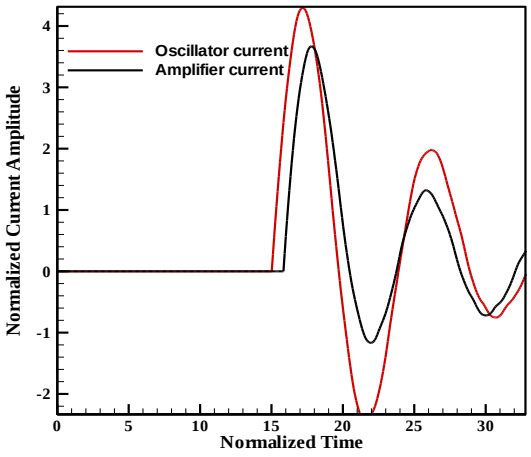

Figure 6. The laser channel currents waveforms variations (OSC & AMP) with L_s = 20nH, $l_{RO} = 0.2m$ and $l_{LA} = 0.8m$.

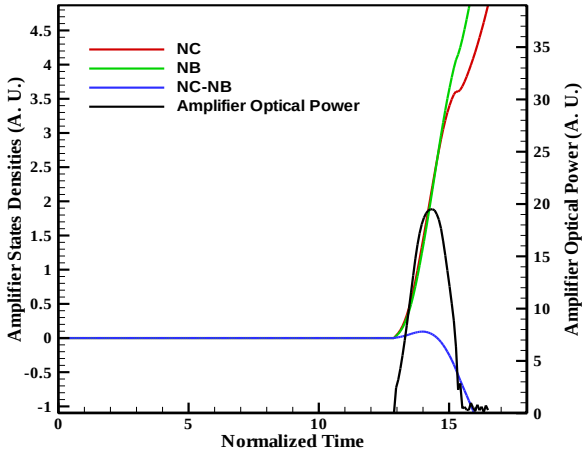

Figure 8. Shows $N_C, N_B, N_C - N_B$ and amplifier optical power waveforms.

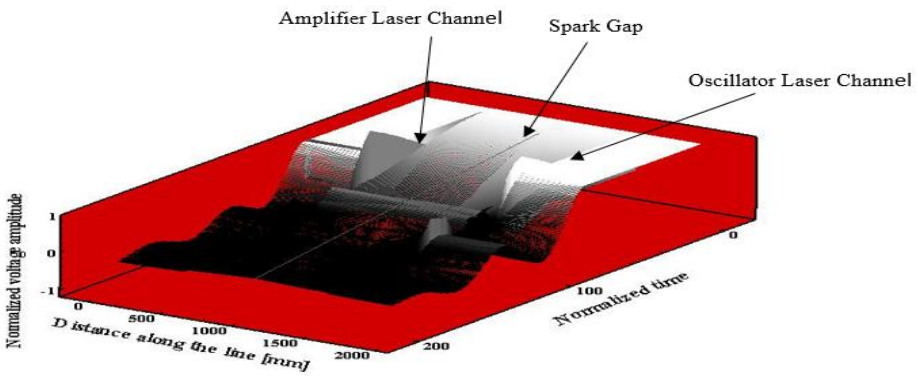

ISSN 1737-9296

Figure 9. A 3-D voltage waveform variations at all points and at any time along the DBL Line N_2 laser.

Figure 8 shows the waveforms of the density of the C-state, the B-state, and the optical power, as well as the density difference between the C and B states in the amplifier laser channel. The density of the C-state is appeared to be higher than that of the B-state for the first time span after the breakdown (~2.5Tr), then the density of the B-sates becomes higher for the rest of the time. This behaviour, however, is due to both the short lifetime of the C-state and the long lifetime of the B-state, and the density difference curves show this behaviour. The optical waveform of the amplifier shown in figure 8 represents the output as if the amplifier were not synchronized with the oscillator, however, the output would be increased if the reflecting mirror were arranged according to the computed synchronization time between the channel peak currents of the (OSC-AMP). For example, if the time difference between the two current peaks is 8ns, and since the transmission line length between the laser channels is 1m, and the phase velocity of the free space is $3x10^8$ m/s, the pulse will take 3.3333ns to travel from the OSC laser channel to the AMP laser channel, leaving 4.6670ns for reflector mirrors, which means 0.7m separation from the double Blumlein circuit for each mirror. That's the required time to align the output oscillator pulse with the peak value of the amplifier laser channel current. If the time between the current peaks changed, it would be better to change the mirror arrangements to make sure that the oscillator optical output reaches the amplifier channel while all the N2 molecules are excited and occupy the higher energy C state. The 3D voltage waveform variations at all points and at any time along the DBL circuit (OSC-AMP) using the DPM model is shown in figure 9.

VI. Conclusions

In this paper we present a full distributed parameter model of the Double-Blumlein-line N2 laser with the use of decoupling approach of the laser rate equations from the electrical circuit equations that make the optical waveforms computations more simple. The electrical equations were first simulated in separate to obtain the voltages, currents waveforms variations. The effect of the transmission-line lengths, the spark gap inductance and the laser gap inductance on the output waveforms variations were carried out. The investigation results showed that the synchronization time between the OSC and AMP was highly affected by those parameters variations. Second, the optical power waveform of the amplifier was obtained by simulating the laser rate equations under the generalized condition in conjunction with the use of (E/P) values resulting from the simulation of electrical equations without using the reflected mirrors arrangements for synchronization. However, it is clear that the peak value of the amplifier optical power would be enhanced and amplified if the reflected mirrors arrangements for synchronization were considered.

Perhaps one of the most important result of this paper is that the mathematical model and the approach developed here could be used to optimize the (OSC-AMP) nitrogen laser system synchronization time, and to improve its performance over a wide range of parametric variations, since the computations here are based on the DPM, and the DPM was proved to be more accurate than convenient LPM. Also, in this model of the DBL, the synchronization could be achieved by using only one spark gap without the need of adding another spark gap with a precise triggering circuits to synchronize the oscillator output with the peak amplifier discharge current, and/or by varying the AMP gas-pressure appropriately to reach the synchronization time condition between OSC and AMP. I think the analysis presented here is quite general and could be applied to many other DBL (OSC-AMP) gas laser systems such as Cu-vapor, TEA CO2 laser, etc. Further experimental research will be pursued aimed at verifying the theoretical results experimentally and determining the optimum operating condition of the DBL (OSC-AMP) circuit.

References

[1] S. Panahibakhsh, S. Sarikhani, and A. Hariri, "Experimental and theoretical investigations for describing pressure dependence of amplified spontaneous emission output energy, small signal gain and electrical conductivity in nitrogen lasers," *Optik*, vol. 168, pp. 541–552, Sep. 2018.

[2] A.W. DeSilva, J.D. Sethian, and J. D. Sethiana, "A pulsed nitrogen laser for optical plasma diagnostics," Naval Research Laboratory, NRL Memorandum Report 6893, 1991.

[3] A. Hariri, M. Jaberi, and S. Ghoreyshi, "Nitrogen lasers: Optical devices of variable gain coefficient," *Opt. Commun*., vol. 281, pp. 3841–3852, Mar. 2008.

[4] Mohamed O. Twati, A. Ben Otman, "Distributed parameter analysis of a Blumlein-Line N2 Laser," *Opt. Commun.*, vol. 99, pp. 405-412, Jun. 1993.

ISSN 1737-9296

[5] Mohamed O. Twati, A. Ben Otman, "A Modified Approach for the Blumlein-line Laser Power Calculations: Electrical and Optical Power Waveforms," *Journal of Wireless Communications*, vol. 2, pp.1-6, Feb. 2017.

[6] Fitzsimmons W A, Anderson L W, Riedhauser C E and Vrtilek J M, "Experimental and Theoretical Investigation of the Nitrogen Laser," *IEEE J. Quantum Electron.*, vol. QE-12, pp. 624-633, New York Oct. 1976.

[7] C. R. Chester, *Technique in partial differential equations*, New York, USA: McGraw-Hill, 1971.

ISSN 1737-9296